

# Arrested states of solids

Madan Rao\*<sup>†</sup> and Surajit Sengupta\*\*<sup>§</sup>

\*Raman Research Institute, C.V. Raman Avenue, Sadashivanagar, Bangalore 560 080, India

\*\*Material Science Division, Indira Gandhi Center for Atomic Research, Kalpakkam 603 102, India

<sup>§</sup>Current address: Institut für Physik, Johannes Gutenberg Universität Mainz, 55099 Mainz, Germany

Solids produced as a result of a fast quench across a freezing or a structural transition get stuck in long-lived metastable configurations of distinct morphology, sensitively dependent on the processing history. *Martensites* are particularly well-studied examples of nonequilibrium solid–solid transformations. Since there are some excellent reviews on the subject, we shall, in this brief article, mainly present our viewpoint.

## Nonequilibrium structures in solids

What determines the final microstructure of a solid under changes of temperature or pressure? This is a complex issue, since a rigid solid finds it difficult to flow along its free energy landscape to settle into a unique equilibrium configuration. Solids often get stuck in long-lived metastable or jammed states because the energy barriers that need to be surmounted in order to get unstuck are much larger than  $k_B T$ .

Such nonequilibrium solid structures may be obtained either by quenching from the liquid phase across a freezing transition (see Caroli *et al.*<sup>1</sup> for a comprehensive review), or by cooling from the solid phase across a structural transition. Unlike the former, nonequilibrium structures resulting from structural transformations do not seem to have attracted much attention amongst physicists, apart from Barsch *et al.*<sup>2</sup> and Gooding *et al.*<sup>3</sup>, possibly because the microstructures and mechanical properties obtained appear nongeneric and sensitively dependent on details of processing history.

Metallurgical studies have however classified some of the more generic nonequilibrium microstructures obtained in solid (parent/austenite)–solid (product/ferrite) transformations depending on the kind of shape change and the mobility of atoms. To cite a few:

- *Martensites* are the result of solid state transformations involving shear and no atomic transport. Martensites occur in a wide variety of alloys, polymeric solids and ceramics, and exhibit very distinct plate-like structures built from twinned variants of the product.
- *Bainites* are similar to martensites, but in addition possess a small concentration of impurities (e.g. carbon in iron) which diffuse and preferentially dissolve in the

parent phase.

- *Widmanstätten ferrites* result from structural transformations involving shape changes and are accompanied by short-range atomic diffusion.
- *Pearlites* are an eutectic mixture of bcc Fe and the carbide consisting of alternating stripes.
- *Amorphous* alloys, a result of a fast quench, typically possess some short range ordering of atoms.
- *Polycrystalline* materials of the product phase are a result of a slower quench across a structural transition and display macroscopic regions of ordered configurations of atoms separated by grain boundaries.

That the morphology of a solid depends on the detailed dynamics across a solid–solid transformation, has been recognized by metallurgists who routinely use time–temperature–transformation (TTT) diagrams to determine heat treatment schedules. The TTT diagram is a family of curves parametrized by a fraction of transformed product. Each curve is a plot of the time required to obtain versus temperature of the quench (Figure 1). The TTT curves for an alloy of fixed composition may be viewed as a ‘kinetic phase diagram’. For example, starting from a hot alloy at

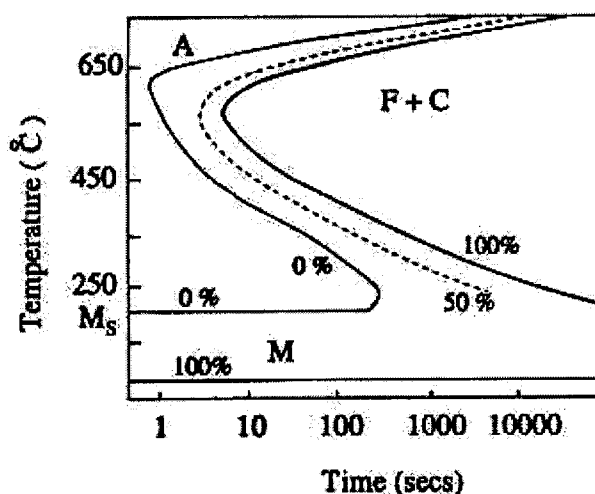


Figure 1. TTT curves<sup>11</sup> for steel AISI 1090 (0.84%C + 0.60% Mn). A: austenite (fcc), F: ferrite (bcc), C: carbide (Fe<sub>3</sub>C). Curves correspond to 0, 50 and 100% transformation. Below a temperature  $M_s$ , the metastable martensite (M) is formed – the transformation curves for martensites are horizontal.

<sup>†</sup>On leave of absence from Institute of Mathematical Sciences, CIT Campus, Taramani, Chennai 600 113, India.

<sup>§</sup>For correspondence. (e-mail: madan@rri.ernet.in)

$t = 0$  equilibrated above the transition temperature (upper left corner) one could, depending on the quench rate (obtained from the slope of a line  $T(t)$ ), avoid the nose of the curve and go directly into the martensitic region or obtain a mixture of ferrite and carbide when cooled slowly.

It appears from these studies that several qualitative features of the kinetics and morphology of microstructures are common to a wide variety of materials. This would suggest that there must be a set of general principles underlying such nonequilibrium solid–solid transformations. Since most of the microstructures exhibit features at length scales ranging from 100 Å to 100 μm, it seems reasonable to describe the phenomenon at the mesoscopic scale, wherein the solid is treated as a continuum. Such a coarse-grained description would ignore atomic details and instead involve effective continuum theories based on symmetry principles, conservation laws and broken symmetry.

Let us state the general problem in its simplest context. Consider a solid state phase diagram exhibiting two different equilibrium crystalline phases separated by a first order boundary (Figure 2). An adiabatically slow quench from  $T_{in} \gg T_{fin}$  across the phase boundary in which the cooling rate is so small that at any instant the solid is in equilibrium corresponding to the instantaneous temperature would clearly result in an equilibrium final product at  $T_{fin}$ . On the other hand, an instantaneous quench would result in a metastable product bearing some specific relation to the parent phase. The task is to develop a nonequilibrium theory of solid state transformations which would relate the nature of the final arrested state and the dynamics leading to it to the type of structural change, the quench rate and the mobility of atoms.

In this article, we concentrate on the dynamical and structural features of a class of solid–solid transformations called *Martensites*. Because of its commercial importance, martensitic transformations are a well-studied field in metallurgy and materials science. Several classic review articles and books discuss various aspects of martensites in great detail<sup>4</sup>. The growing literature on the subject is a clear indication that the dynamics of solid state transformations is still not well understood. We would like to take this opportunity to present, for discussion and criticism, our point of view on this very complex area of nonequilibrium physics<sup>5,6</sup>.

We next review the phenomenology of martensites and highlight generic features that need to be explained by a nonequilibrium theory of solid state transformations.

### Phenomenology of martensites

One of the most studied alloys undergoing martensitic transformations is iron–carbon<sup>4</sup>. As the temperature is reduced, Fe with less than 0.02% C undergoes an equilibrium structural transition (Figure 2) from fcc (austenite) to bcc (ferrite) at  $T_c = 910^\circ\text{C}$ . An adiabatic cooling across  $T_c$

nucleates a grain of the ferrite which grows isotropically, leading to a polycrystalline bcc solid. A faster quench from  $T_{in} > T_c$  to  $T_{fin} < M_s < T_c$  (where  $M_s$ : martensite start temperature) instead produces a rapidly transformed metastable phase called the martensite, preempting the formation of the equilibrium ferrite. It is believed that martensites form by a process of heterogeneous nucleation. On nucleation, martensite ‘plates’ grow radially with a constant front velocity  $\sim 10^5$  cm/s, comparable to the speed of sound. Since the transformation is not accompanied by the diffusion of atoms, either in the parent or the product, it is called a diffusionless transformation. Electron microscopy reveals that each plate consists of an alternating array of twinned or slipped bcc regions of size  $\sim 100$  Å. Such martensites are called acicular martensites.

The plates grow to a size of approximately 1 μm before they collide with other plates and stop. Most often the nucleation of plates is athermal; the amount of martensite nucleated at any temperature is independent of time. This implies that there is always some retained fcc, partitioned by martensite plates. Optical micrographs reveal that the jammed plates lie along specific directions known as habit planes. Martensites, characterized by such a configuration of jammed plates, are long lived since the elastic energy barriers for reorganization are much larger than  $k_B T$ .

A theoretical analysis of the dynamics of the martensitic transformation in Fe–C is complicated by the fact that the deformation is 3-dimensional (Bain strain) with 3 twin variants of the bcc phase. Alloys like In–Tl, In–Pb and Mn–Fe however, offer the simplest examples of martensitic transformations having only two twin variants. In–Tl alloys undergo a tetragonal to orthorhombic transformation when cooled below  $72^\circ\text{C}$  (ref. 2). The orthorhombic phase can be obtained from the tetragonal phase by a two-dimensional deformation, essentially a square to rhombus transition. Experiments indicate that all along the kinetic pathway, the local configurations can be obtained from a two-dimensional deformation of the tetragonal cell. This would imply that the movement of atoms is strongly anisotropic and confined to the  $ab$ -plane. Thus as far as the physics of this transformation is concerned, the  $ab$ -planes are in perfect registry (no variation of the strain along the  $c$ -axis). In the next two sections we shall discuss our work on the dynamics of the square to a rhombus transformation in 2-dimensions using a molecular dynamics simulation and a coarse-grained mode coupling theory.

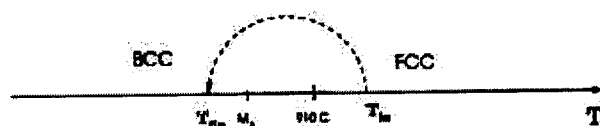


Figure 2. Phase diagram of Fe–C (weight per cent of C < 0.02%).  $M_s$  is the martensite start temperature.

### Molecular dynamics simulation of solid–solid transformations

Our aim in this will be to study the simplest molecular dynamics (MD) simulation of the square to rhombus transformation. We would like to use the simulation results to construct the complete set of coarse grained variables needed in a continuum description of the dynamics of solid state transformations. We carry out the MD simulation in the constant  $NVT$  ensemble using a Nosé–Hoover thermostat ( $N = 12000$ )<sup>7</sup>.

Our MD simulation is to be thought of as a ‘coarse-grained’ MD simulation, where the effective potential is a result of a complicated many-body interaction. One part of the interaction is a purely repulsive two-body potential  $V_2(r_{ij}) = v_2/r_{ij}^{12}$ , where  $r_{ij}$  is the distance between particles  $i$  and  $j$ . The two-body interaction favours a triangular lattice ground state. In addition, triplets of particles interact via a short-range three-body potential  $V_3(\mathbf{r}_i, \mathbf{r}_j, \mathbf{r}_k) = v_3 w(r_{ij}, r_{jk}, r_{ik}) [\sin^2(4_{ijk}) + \sin^2(4_{jki}) + \sin^2(4_{kij})]$ , where  $w(r)$  is a smooth short-range function and  $4_{ijk}$  is the bond angle at  $j$  between particles  $(ijk)$ . Since  $V_3$  is minimized when  $4_{ijk} = 0$  or  $\pi/2$ , the three-body term favours a square lattice ground state. Thus at sufficiently low temperatures, we can induce a square to triangular lattice transformation by tuning  $v_3$ . The phase diagram in the  $T-v_3$  plane is shown in Figure 3.

We define elastic variables, coarse-grained over a spatial block of size  $\lambda$  and a time interval  $\tau$ , from the instantaneous positions  $\mathbf{u}$  of the particles. These include the deformation tensor  $\hat{C}_{ij}/\hat{C}_{ij}^k$ , the full nonlinear strain  $\epsilon_{ij}$ , and the vacancy field  $\rho = \bar{\rho} - \rho_{\text{local}}$  ( $\bar{\rho}$  = coarse-grained local density,  $\bar{\rho}$  = average density). We have kept track of the time dependence of these coarse-grained fields during the MD simulation.

Consider two ‘quench’ scenarios—a high and low temperature quench (upper and lower arrows in Figure 3 respectively) across the phase boundary. In both cases the solid is initially at equilibrium in the square phase.

The high temperature quench across the phase boundary, induces a homogeneous nucleation (i.e. strain inhomogeneities created by thermal fluctuations are sufficient to induce critical nucleation) and growth of a triangular region. The product nucleus grows isotropically with the size  $R \sim t^{1/2}$ . A plot of the vacancy/interstitial fields shows that, at these temperatures they diffuse fast to their equilibrium value (vacancy diffusion obeys an Arrhenius form  $Dv = D_0 \exp(-A/k_B T)$ , where  $A$  is an activation energy, and so is larger at higher temperatures). The final morphology is a polycrystalline triangular solid.

The low temperature quench on the other hand, needs defects (either vacancies or dislocations) to seed nucleation in an appreciable time. This heterogeneous nucleation

initiates an embryo of triangular phase, which grows anisotropically along specific directions (Figure 4). Two aspects are immediately apparent, the growing nucleus is twinned and the front velocities are high. Indeed, the velocity of the front is a constant and roughly half the velocity of longitudinal sound. A plot of the vacancy/interstitial field shows a high concentration at the parent–product interface. The vacancy field now diffuses very slowly and so appears to get stuck to the interface over the time scale of the simulation. If we force the vacancies and interstitials to annihilate each other, then the anisotropic twinned nucleus changes in the course of time to an isotropic untwinned one!

Therefore the lessons from the MD simulation are: (i) There are two scenarios of nucleation of a product in a parent depending on the temperature of quench. The product grows via homogeneous nucleation at high  $T$ , and via heterogeneous nucleation at low  $T$ . (ii) The complete set of slow variables necessary to describe the nucleation of solid–solid transformations should include the strain tensor and defects (vacancies and dislocations) which are generated at the parent–product interface at the onset of nucleation. (iii) The relaxation times of these defects dictate the final morphology. At high temperatures the defects relax fast and the grains grow isotropically with a diffusive front. The final morphology is a polycrystalline triangular solid. At low temperatures, the interfacial defects (vacancies) created by the nucleating grain relax slowly and get stuck at the parent–product interface. The grains grow anisotropically along specific directions. The critical nucleus is twinned and the front grows ballistically (with a velocity comparable to the sound speed). The final morphology is a twinned martensite.

### Mode coupling theory of solid–solid transformations

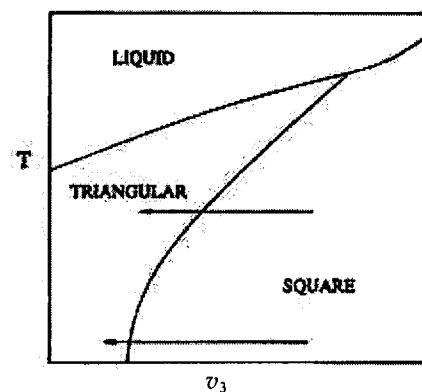
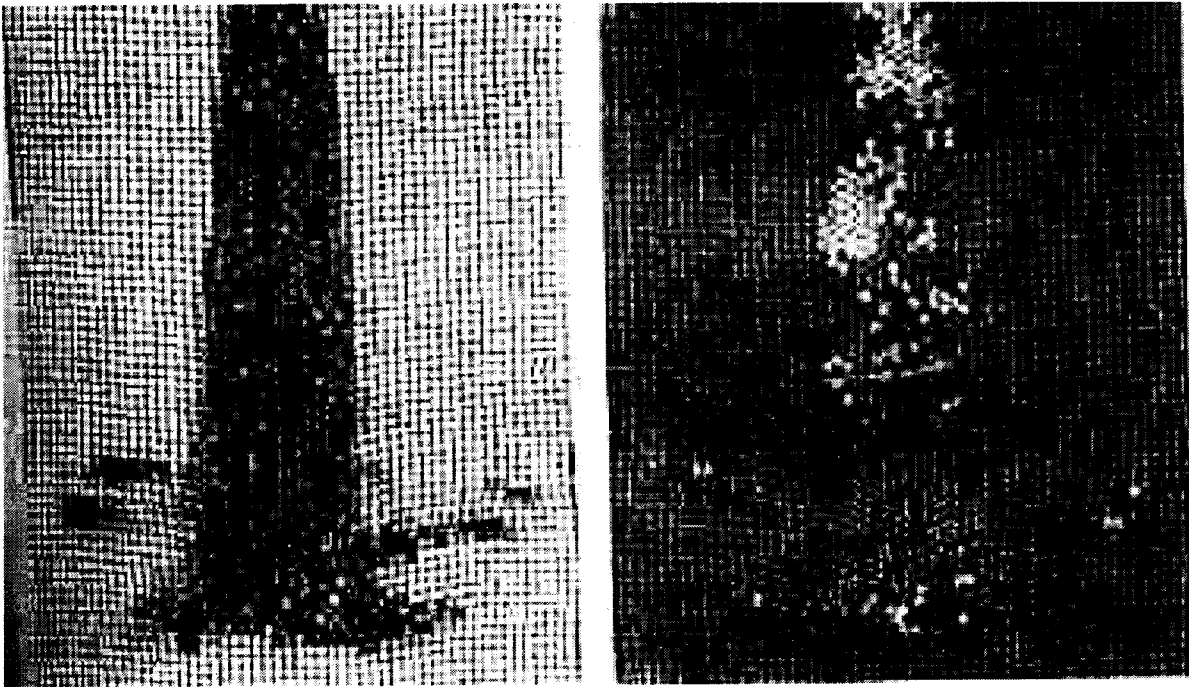


Figure 3.  $T-v_3$  phase diagram from the MD simulations showing the freezing and structural transitions. The upper and lower arrows correspond to the high and low temperature quenches, respectively.



**Figure 4.** MD snapshot of (a) the nucleating grain at some intermediate time initiated by the low temperature quench across the square-triangle transition. The dark (white) region is the triangular (square) phase, respectively. Notice that the nucleus is twinned and highly anisotropic. (b) The vacancy (white)/interstitial (black) density profile at the same time as a. Notice that the vacancies and interstitials are well separated and cluster around the parent-product interface.

Armed with the lessons from the MD simulation, let us now construct a continuum elastic theory of solid-state nucleation. The analysis follows in part the theories of Krumhansl *et al.*<sup>2</sup>, but has important points of departure. The procedure is to define a coarse grained free energy functional in terms of all the relevant ‘slow’ variables. From the simulation results, we found that every configuration is described in terms of the local (nonsingular) strain field  $\epsilon_{ij}$ , the vacancy field  $v$ , and singular defect fields like the dislocation density  $b_{ij}$ . These variables are essentially related to the phase and amplitudes of the density wave describing the solid  $\{ \mathbf{c} \}$ .

It is clear from the simulation that the strain tensor, defined with respect to the ideal parent, gets to be of  $O(1)$  in the interfacial region between the parent and the product. Thus we need to use the full nonlinear strain tensor  $\epsilon_{ij} = (\hat{\mu}_j + \hat{\mu}_i + \hat{\mu}_k \hat{\mu}_k) / 2$ . Further, since the strain is inhomogeneous during the nucleation process, the free energy functional should have derivatives of the strain tensor  $\hat{\epsilon}_{kij}$  (this has unfortunately been termed ‘nonlocal strain’ by some authors).

In general, the form of the free energy functional can be very complicated, but in the context of the square-to-rhombus transformation, the free energy density may be approximated by a simple form,

$$f = c(\epsilon_{11})^2 + \epsilon_{11}^2 - a^4 + \epsilon_{11}^6 + v^2 + d b^2 + k_d b \quad (1)$$

where  $\epsilon_{11}$  is the nonzero component of the strain

corresponding to the transformation between a square and a rhombus,  $v$  is the vacancy field and  $b$  is the (scalar) dislocation density. The tuning parameter  $a$  induces a transition from a square (described by  $\epsilon_{11} = 0$ ) to a rhombus ( $\epsilon_{11} = \epsilon_0$ ).

Starting with  $\epsilon_{11} = 0$  corresponding to the equilibrium square parent phase at a temperature  $T > T_c$ , we quench across the structural transition. The initial configuration of  $\epsilon_{11}$  is now metastable at this lower temperature, and would decay towards the true equilibrium configuration by nucleating a small ‘droplet’ of the product. As we saw in the last section, as soon as a droplet of the product appears embedded in the parent matrix, atomic mismatch at the parent-product interface gives rise to interfacial defects like vacancies and dislocations.

Let us confine ourselves to solids for which the energy cost of producing dislocations is prohibitively large. This would imply that the interfacial defects consist of only vacancies and interstitials. The dynamics of nucleation now written in terms of  $\epsilon_{11}$ ,  $\mathbf{g}$  (the conserved momentum density) and vacancy  $v$  are complicated<sup>5</sup>. For the present purpose, all we need to realize is that  $\epsilon_{11}$  couples to the strain and is diffusive with a diffusion coefficient  $D_v$  depending on temperature.

As in the MD simulation, we find that the morphology and growth of the droplet of the product depends critically on the diffusion of these vacancies. If the temperature of quench is high,  $\epsilon_{11}$  diffuses to zero before the critical nucleus

size is attained and the nucleus eventually grows into an equilibrium (or polycrystalline) triangular solid. In this case, the nucleus grows isotropically with  $R \sim t^{1/2}$ . However, a quench to lower temperatures results in a low vacancy diffusion coefficient. In the limit  $D_v \ll 0$ , the  $v$ -field remains frozen at the moving parent-product interface. In this case, a constrained variational calculation of the morphology of the nucleus shows that it is energetically favourable to form a twinned martensite rather than a uniform triangular structure. The growth of the twinned nucleus is not isotropic, but along habit planes. Lastly, the growth along the longer direction is ballistic with a velocity proportional to  $(\sigma_{pp})^{1/2}$  (of the order of the sound velocity). All these results are consistent with the results of the previous section and with martensite phenomenology. Let us try and understand in more physical terms, why the growing nucleus might want to form twins.

As soon as a droplet of the triangular phase of dimension  $L$  is nucleated, it creates vacancies at the parent-product interface. The free energy of such an inclusion is  $F = F_{\text{bulk}} + F_{\text{pp}} + F$ . The first term is simply the bulk free energy gain equal to  $\sigma F^2$ , where  $\sigma F$  is the free energy difference between the square and triangular phases. The next two terms are interfacial terms.  $F_{\text{pp}}$  is the elastic contribution to the parent-product interface coming from the gradient terms in the free energy density eq. (1), and is equal to  $4\sigma_{\text{pp}}L$ , where  $\sigma_{\text{pp}}$  is the surface tension at the parent-product interface.  $F$  is the contribution from the interfacial vacancy field glued to the parent-product interface and is proportional to  $\sigma^2 \sim L^2$  (since the atomic mismatch should scale with the amount of parent-product interface). This last contribution dominates at large  $L$  setting a prohibitive price to the growth of the triangular nucleus. The solid gets around this by nucleating a twin with a strain opposite to the one initially nucleated, thereby reducing  $\sigma$ . Indeed for an equal size twin,  $\sigma \ll 0$  on the average, and leads to a much lower interfacial energy  $F \sim L$ . However, the solid now pays the price of having created an additional twin interface whose energy cost is  $F_{\text{tw}} = \sigma_{\text{tw}}L$ .

Considering now an (in general) anisotropic inclusion of length  $L$ , width  $W$  consisting of  $N$  twins, the free energy calculation goes as

$$F = \sigma FLW + \sigma_{\text{pp}}(L + W) + \sigma_{\text{tw}}NW + (L/N)^2 \sigma^2$$

where the last term is the vacancy contribution. Minimization with respect to  $N$  gives  $L/N \sim W^{1/2}$ , a relation that is well known for 2-dimensional martensites like In-Tl.

Our next task is to solve the coupled dynamical equations with appropriate initial conditions numerically, to obtain the full morphology phase diagram as a function of the type of structural change, the parameters entering the free energy functional and kinetic parameters like  $D_v$ .

It should be mentioned that our theory takes off from the

theories of Krumhansl *et al.*<sup>2</sup>, in that we write the elastic energy in terms of the nonlinear strain tensor and its derivatives. In addition, we have shown that the process of creating a solid nucleus in a parent generates interfacial defects which evolve in time. The importance of defects has been stressed by a few metallurgists<sup>8</sup>. We note also that the parent-product interface is studded with an array of vacancies with a separation equal to the twin size. This implies that the strain decays exponentially from the interface over a distance of order  $L/N$ . This has been called 'fringing field'<sup>2</sup>. They obtain this by imposing boundary conditions on the parent-product interface, whereas here it appears dynamically.

### Patterning in solid-solid transformations: Growth and arrest

So far we have discussed the nucleation and growth of single grains. This description is clearly valid at very early times, for as time progresses the grains grow to a size of approximately 1  $\mu\text{m}$  and start colliding, whereupon in most alloys they stop. Optical micrographs of acicular martensites reveal that the jammed plates lie along habit planes that criss-cross and partition the surrounding fcc (parent) matrix.

Can we quantify the patterning seen in martensite aggregates over a scale of a millimeter? A useful measure is the size distribution of the martensite grains embedded in a given volume of the parent. The appropriate (but difficult!) calculation at this stage would be the analogue of a Becker-Döring theory for nucleation in solids. In the absence of such a theory, we shall take a phenomenological approach.

Clearly the size distribution  $P(l, t)$  depends on the spatio-temporal distribution  $I$  of nucleation sites and the growth velocity  $v$ . We have analysed the problem explicitly in a simple 2-dimensional context. Since the nucleating martensitic grains are highly anisotropic and grow along certain directions with a uniform velocity, a good approximation is to treat the grains as lines or rays. These rays (lines) emanate from nucleation sites along certain directions, and grow with a constant velocity  $v$ . The rays stop on meeting other rays and eventually after a time  $T$ , the 2-dimensional space is fragmented by  $N$  colliding rays. The size distribution of rays, expressed in terms of a scaling variable  $y = y(l, v)$ , has two geometrical limits – the  $l$ -fixed point (at  $y = 0$ ) and the  $L$ -fixed point (at  $y = \infty$ ). The  $l$ -fixed point corresponds to the limit where the rays nucleate simultaneously with a uniform spatial distribution. The stationary distribution  $P(l)$  is a Gamma distribution with an exponentially decaying tail. The  $L$ -fixed point, corresponds to the limit where the rays are nucleated sequentially in time (and uniformly in space) and grow with infinite velocity. By mapping on to a multifragmentation problem, Ben Naim and Krapivsky<sup>9</sup> were able to derive the exact asymptotic form for the moments of  $P(l)$  at the  $L$ -fixed point. The distribution

function  $P(l)$  has a multiscaling form, characterized by its moments  $\langle l^q \rangle \sim N^{-\phi(q)}$ , where  $\phi(q) = (q + 2 - (q^2 + 4)^{1/2})/2$ . At intermediate values of the scaling variable  $y$ , there is a smooth crossover from the  $\square$ -fixed point to the  $L$ -fixed point with a kinematical crossover function and crossover exponents.

The emergence of scale invariant microstructures in martensites as arising out of a competition between the nucleation rate and growth is a novel feature well worth experimental investigation. There have been similar suggestions in the literature, but as far as we know there have been no direct visualization studies of the microstructure of acicular martensites using optical micrographs. Recent acoustic emission experiments<sup>10</sup> on the thermoelastic reversible martensite Cu–Zn–Al, may be argued to provide indirect support of the above claim<sup>5</sup>, but the theory of acoustic emission in martensites is not understood well enough to make such an assertion with any confidence.

### Open questions

We hope this short review makes clear how far we are in our understanding of the dynamics of solid–solid transformations. A deeper understanding of the field will only come about with systematic experiments on carefully selected systems. For instance, a crucial feature of our nonequilibrium theory of martensitic transformations is the existence of a dynamical interfacial defect field. In conventional Fe based alloys, the martensitic front grows incredibly fast, making it difficult to test this using *in situ* transmission electron microscopy. Colloidal solutions of polystyrene spheres (polyballs) however, are excellent systems for studying materials properties. Polyballs exhibiting fcc  $\times$  bcc structural transitions have been seen to undergo twinned martensitic transformations. The length and time scales associated with colloids are large, making it comfortable to study these systems using light scattering and optical microscopy.

In this article we have focused on a small part of the dynamics of solid state transformations, namely the dynamics and morphology of martensites. Even so our presentation here is far from complete and there are crucial unresolved questions that we need to address.

Let us list the issues as they appear following a nucleation event.

The physics of heterogeneous nucleation in solids is very poorly understood. For instance, it appears from our simulations that the morphology of the growing nucleus depends on the nature of the defects seeding the nucleation process (e.g. vacancies, dislocations and grain

boundaries). In addition, several martensitic transformations are associated with correlated nucleation events and autocatalysis. Though these features are not central to the

issue of martensites, such a study would lead to a better understanding of the origins of athermal, isothermal and burst nucleation. This in conjunction with a ‘Becker–Döring theory’ for multiple martensite grains would be a first step towards the computation of TTT curves.

We still do not understand the details of the dynamics of twinning and how subsequent twins are added to the growing nucleus. Moreover, the structure and dynamics of the parent–product interface and of the defects embedded in it have not been clearly analysed.

It would be desirable to have a more complete theory which displays a morphology phase diagram (for a single nucleus) given the type of structural transition and the kinetic, thermal and elastic parameters.

Certain new directions immediately suggest themselves. For instance, the role of carbon in interstitial alloys like Fe–C leading to the formation of *bainites*; the coupling of the strain to an external stress and the *shape memory* effect; tweed phases and pre-martensitic phenomena (role of quenched impurities).

The study of the dynamics of solid–solid transformations and the resulting long-lived morphologies lies at the intersection of metallurgy, materials science and nonequilibrium statistical mechanics. The diversity of phenomena makes this an extremely challenging area of nonequilibrium physics.

1. Caroli, B., Caroli, C. and Roulet, B., in *Solids Far from Equilibrium* (ed. Godreche, C.), Cambridge University Press, 1992.
2. Barsch, G. R. and Krumhansl, J. A., *Phys. Rev. Lett.*, 1974, **37**, 9328; Barsch, G. R., Horovitz, B. and Krumhansl, J. A., *Phys. Rev. Lett.*, 1987, **59**, 1251.
3. Bales, G. S. and Gooding, R. J., *Phys. Rev. Lett.*, 1991, **67**, 3412; Reed, A. C. E. and Gooding, R. J., *Phys. Rev.*, 1994, **B50**, 3588; van Zyl, B. P. and Gooding, R. J., <http://xxx.lanl.gov/archive/cond-mat/9602109>.
4. Roitburd, A., in *Solid State Physics* (eds Seitz and Turnbull), Academic Press, NY, 1958; Nishiyama, Z., *Martensitic Transformation*, Academic Press, NY, 1978; Kachaturyan, A. G., *Theory of Structural Transformations in Solids*, Wiley, NY, 1983; *Martensite* (eds Olson, G. B. and Owen, W. S.), ASM International, The Materials Information Society, 1992.
5. Rao, M. and Sengupta, S., *Phys. Rev. Lett.*, 1997, **78**, 2168; Rao, M. and Sengupta, S., *lanl e-print: cond-mat/9709022*; Rao, M. and Sengupta, S., *IMSc preprint*, 1998.
6. Rao, M., Sengupta, S. and Sahu, H. K., *Phys. Rev. Lett.*, 1995, **75**, 2164; Rao, M. and Sengupta, S., *Phys. Rev. Lett.*, 1996, **76**, 3235; Rao, M. and Sengupta, S., *Physica A*, 1996, **224**, 403.
7. Sengupta, S. and Rao, M., to be published.
8. Olson, G. B. and Cohen, M., *Acta Metall.*, 1979, **27**, 1907; Olson, G. B., *Acta Metall.*, 1981, **29**, 1475; Christian, J. W., *Metal. Trans. A*, 1982, **13**, 509.
9. Ben Naim, E. and Krapivsky, P., *Phys. Rev. Lett.*, 1996, **76**, 3235.
10. Vives, E. *et al.*, *Phys. Rev. Lett.*, 1994, **72**, 1694.
11. *Metals Handbook*, ASM, Ohio, 9th edition, vol. 4, 1981.

ACKNOWLEDGEMENT. We thank Yashodhan Hatwalne for a critical reading of the manuscript.